Tunneling Leakage Current Dependent RDD Model Framework for Gate Oxide TDDB

Tarun Samadder and Souvik Mahapatra
Department of Electrical Engineering, Indian Institute of Technology Bombay, Mumbai 400076, India
*Phone: +91-222-572-0408, Email: souvik@ee.iitb.ac.in

Abstract: **The Reaction Diffusion Drift (RDD) model is used to simulate trap generation (ΔN_{TG}) kinetics during Time Dependent Dielectric Breakdown (TDDB) experiments. Several features of measured data, *e.g.*, stress gate voltage (V_G) dependence of mean time to breakdown (T_{BD}) across temperature (T) and gate oxide thickness (Tox), Weibull slope (β) across Tox are explained. The role of electron (J_E) and/ or hole (J_H) leakage current (with J_H from Anode Hole Injection or AHI) is explored as a trigger for RDD model. The polarity gap between positive and negative V_G stress is addressed.**

Keywords: ***Tunneling leakage current, Anode Hole Injection, Reaction Diffusion Drift Model, Time Dependent Dielectric Breakdown.***

I. INTRODUCTION

TDDB is caused by gradual buildup of gate oxide defects, leading to formation of a percolation path between gate and channel and resulting increase in gate leakage current at time T_{BD} [1]-[13]. Percolation path formation is stochastic in nature, and T_{BD} shows Weibull distribution [2]. The V_G dependence of T_{BD} is modeled by different physical mechanisms, *e.g.*, AHI [14], [15], Thermo-Chemical (TC) [16], or Anode Hydrogen Release (AHR) [17]. However, none addressed the trap generation time kinetics (Stress Induced Leakage Current or SILC) and resulting failure when a critical defect density (N_{BD}) is reached. In this paper, a leakage current triggered RDD model is used to address the same and bridge the gap in co-simulation of SILC and TDDB.

II. GATE LEAKAGE CURRENT

Fig.1 shows the band diagrams for (a) Fowler-Nordheim (FN) tunneling and (b) Direct Tunneling (DT) of electrons from cathode to anode via (a) thick and (b) thin gate oxide, energy gain from oxide field, impact ionization to generate holes in anode, and injection of holes into gate oxide for NMOS in (a) inversion (V_G>0) and (b) accumulation (V_G<0) stress. The extra energy gain across the bandgap of the p-type substrate (i.e., minority ionization, Fig.1(b)) results in a higher hole-to-electron current ratio, Fig.2, demonstrating the impact of stress voltage polarity on AHI process [18].

III. RDD MODEL

H-passivated bonds are broken (K_{F1}) via injection of electrons and/or holes, oxide field (E_{OX}) and temperature (T), released H atoms diffuse and subsequently break other bonds to generate H_2 molecules (K_{F2}) and H_2^+, OH^- ions (K_{F3}) that diffuse or drift away, Fig.3. Broken bonds results in bulk traps (density ΔN_{TG}), whose magnitude at a given time is governed by K_{F1}, and long-time power-law time kinetics slope (n) is governed by the relative ratio of molecules to ions (K_{F2}/K_{F3}), Fig.4. The mean T_{BD} is calculated as the time taken to reach N_{BD} [2], [14]. Except K_{F1}, the parameters (reaction rates and diffusivities) are Arrhenius T activated, and except K_{F1} and K_{F30} pre-factor of K_{F3}, all other parameters are kept fixed across all cases studied in this paper.

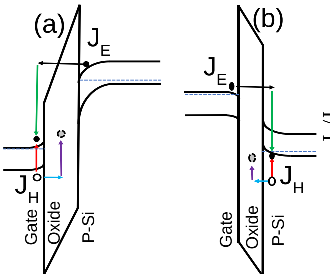

Fig.1 Energy band diagram showing electron tunneling, impact ionization, hole injection into bulk, and defect generation during (a) inversion and (b) accumulation for NMOS capacitor.

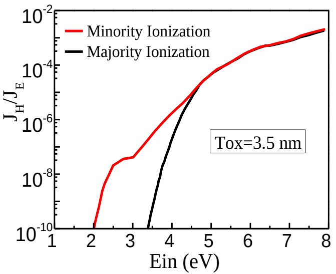

Fig.2 Ratio of hole and electron current density (J_H/J_E) versus injection energy (Ein) [18] showing the impact of bias polarity on majority and minority ionization.

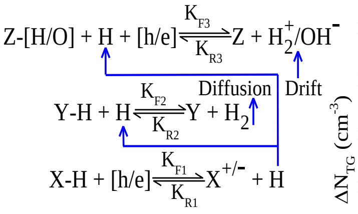

$$K_{F1} = K_{F10}.J_E^m.J_H^p.e^{Eox*(\Gamma_0+\alpha/kT)}.e^{-Ea/kT}$$

Fig.3 RDD model chemical equations showing diffusion of molecular, drift of ionic species, and first interface reaction rate K_{F1} dependence on tunneling leakage current, electric field, and temperature (bottom).

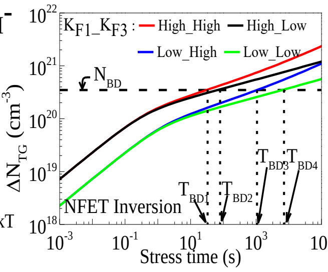

Fig.4 RDD model simulated bulk trap (ΔN_{TG}) kinetics for different K_{F1} (magnitude) and K_{F3} (slope, n) demonstrating different mean time to breakdown (T_{BD}) as it reaches critical defect density (N_{BD}).

IV. PERCOLATION MODEL

Fig.5 plots Weibull β versus Tox from various reports. The percolation model suggests $\beta = n*Tox/a_0$ (a_0 being cell size) [2], [19], the β trend in Fig.5 can be modelled by Tox dependence of *n* and a_0 as shown in Fig.6 and Fig.7 respectively. The *n* values are consistent with reported SILC slopes (after correction for sensing delay related discharging effect) at different Tox, and K_{F30} of RDD model can be varied to vary *n*. The reduction in a_0 at lower Tox is reported elsewhere. Fig.8 plots the Tox dependence of N_{BD} from various reports (with fixed a_0), and calculated by analytical percolation model [19] with fixed a_0 and varying a_0 as per Fig.7. A large N_{BD} reduction at lower Tox is observed for fixed a_0, the reduction of N_{BD} is much less when a_0 reduces at lower Tox.

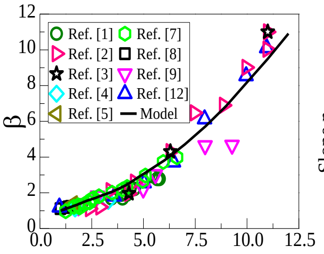

Fig.5 Weibull slope (β) versus oxide thickness (Tox) from various reports and calculation (β=n*Tox/a_0), slope (n) and cell size (a_0) are taken from Fig.6 and Fig.7 trend, respectively.

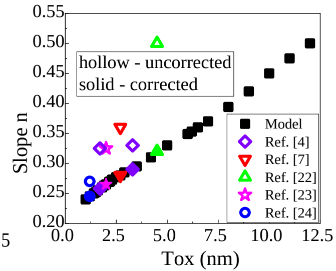

Fig.6 Variation of bulk trap slope (n) and reported SILC slopes (after correction for sensing delay related discharging effect) with oxide thickness (Tox) from various reports and general trends.

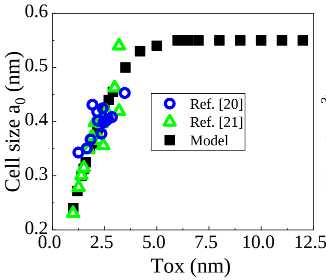

Fig.7 Variation of cell size (a_0) as per percolation model with oxide thickness (Tox) from various reports and general trends.

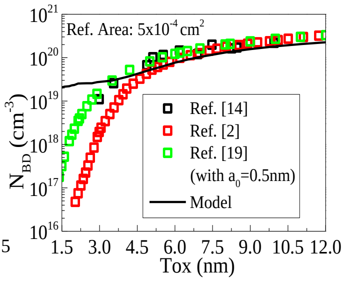

Fig.8 Mean critical defect density (N_{BD}) versus Tox. The Model line is calculated using nine neighbor model of [19] considering Tox dependent a_0 as shown in Fig.7.

V. MODELING OF MEAN T_{BD}

RDD model is used for time kinetics of ΔN_{TG} with K_{F1} related to J_E, J_H, E_{OX} and T, Fig.3, where K_{F10} is the reaction rate pre-factor, Γ_0 is field acceleration factor, α is bond polarization constant and E_A is the activation energy. J_E is calculated either from charge to breakdown (Q_{BD}) data [6], [13] or FN and DT expressions [14], whereas J_H is calculated from the J_H/J_E ratio of AHI model, Fig.2 [18]. The K_{F1} term is generic and covers all physical cases, i.e., TC (m=p=0), AHR (p=0), and AHI (m=0). The experimental and modeled mean T_{BD} versus V_G at a fixed T for various Tox are shown in Fig.9 for NMOS inversion (NI), in Fig.10 for NMOS accumulation (NA), and in Fig.11 for PMOS inversion (PI). The experimental and modeled mean T_{BD} versus V_G at different T are shown in PMOS accumulation (PA) for relatively thin and thick Tox respectively in Fig.12 and Fig.13. In all cases, ΔN_{TG} time kinetics is calculated from RDD model, with a choice of K_{F30} to obtain n for a given Tox as per Fig.7, and T_{BD} is noted when ΔN_{TG}=N_{BD}. The pre-factor K_{F10} is shown versus Tox for all cases (NI, NA, PI, and PA) for different choice of m and p in Fig.14. The variation of K_{F10} with Tox for NA and PI is negligible compared to that for NI and PA which show opposite trends, Fig.14(a), for m=p=0 (TC). For m=0.5 and p=0 (AHR), Fig.14(b), K_{F10} for NI has a decreasing trend with Tox scaling, whereas, for m=0 and p=0.5 (AHI), Fig.14(c), K_{F10} increases with Tox scaling for all cases. K_{F10} for all cases remains almost constant across Tox for m=p=0.3, Fig.14(d), suggesting both J_E and J_H being responsible for initial dissociation of H bonds. A slight difference in K_{F10} is observed between NI versus NA and PI versus PA, which is possibly due to difference in gate oxide quality (~bond strength) near the poly-Si gate (NI and PA) and Si substrate (NA and PI), and doping of gate and substrate.

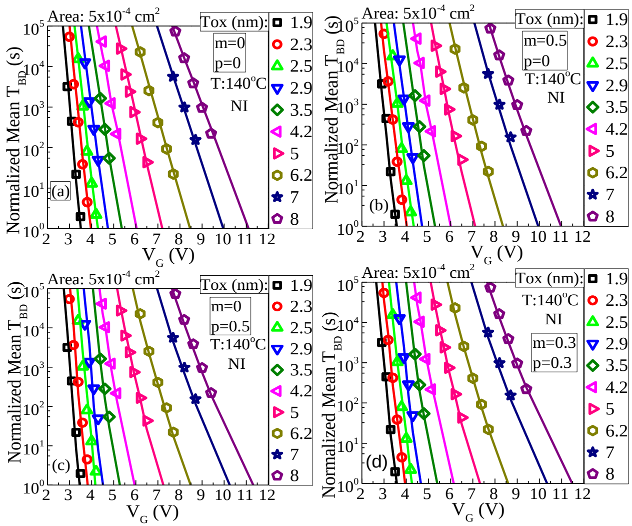

Fig.9 Mean T_{BD} versus V_G at a fixed T for NMOS capacitor with different Tox stressed in inversion with K_{F1} (see the equation at the bottom in Fig.3) taking (a) m=p=0; (b) m=0.5, p=0; (c) m=0, p=0.5; and (d) m=p=0.3. Data (symbols) from [6],[10],[11].

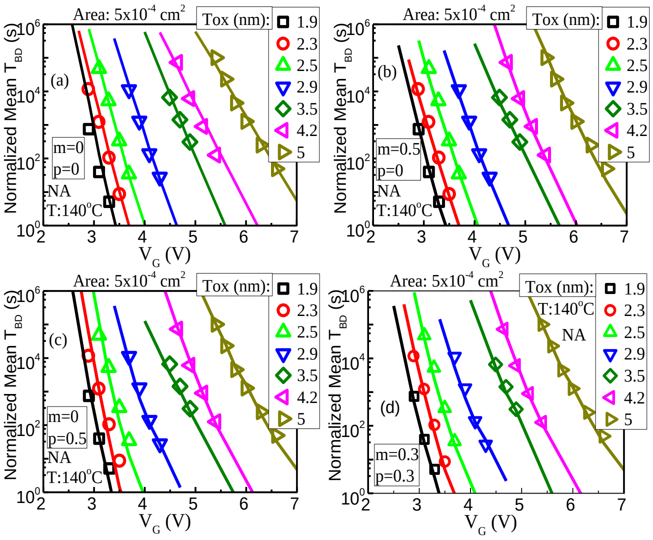

Fig.10 Mean T_{BD} versus V_G at a fixed T for NMOS capacitor in accumulation with different Tox modeled with K_{F1} (see the equation at the bottom in Fig.3) taking (a) m=p=0; (b) m=0.5, p=0; (c) m=0, p=0.5; and (d) m=p=0.3. Data (symbols) from [6].

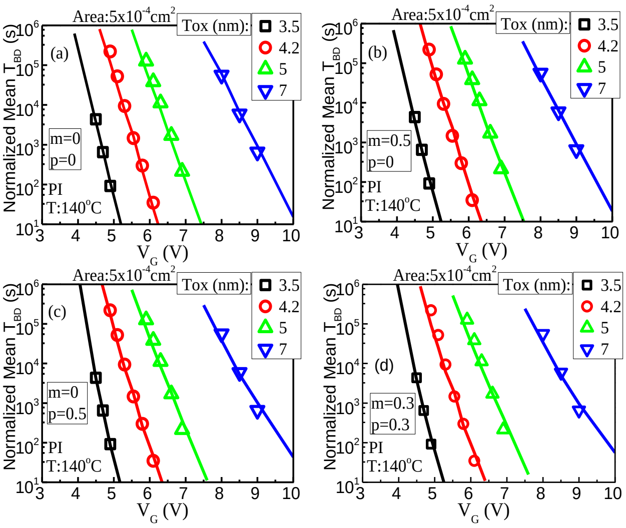

Fig.11 Mean T_{BD} versus V_G at a fixed temperature (T) for PMOS capacitor with different Tox stressed in inversion with K_{F1} (see the equation at the bottom in Fig.3) taking (a) m=p=0; (b) m=0.5, p=0; (c) m=0, p=0.5; and (d) m=p=0.3. Data (symbols) from [10].

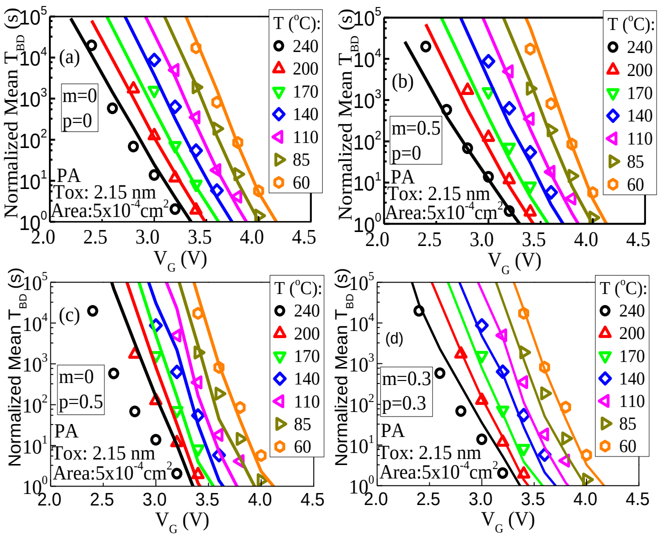

Fig.12 Mean T_{BD} versus stress V_G at different temperatures (T) for thin PMOS capacitor stressed in accumulation (PA) with K_{F1} (see the equation at the bottom in Fig.3) taking (a) m=p=0; (b) m=0.5, p=0; (c) m=0, p=0.5; and (d) m=p=0.3. Data (symbols) from [13].

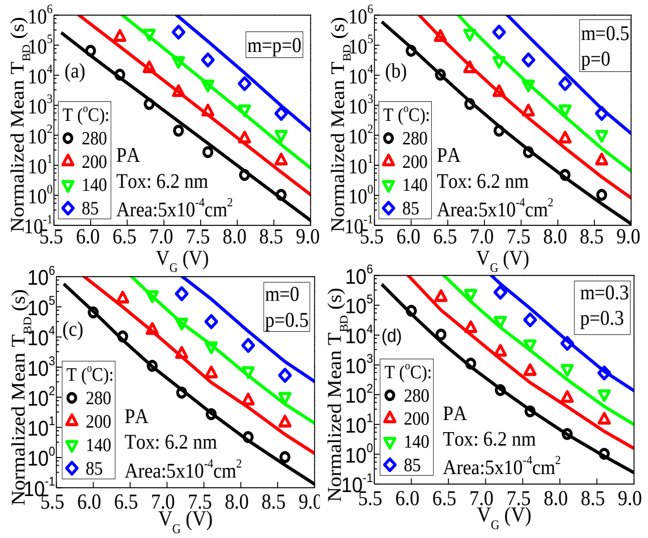

Fig.13 Mean T_{BD} versus V_G at various T for thick PMOS capacitor stressed in accumulation (PA) with K_{F1} (see the equation at the bottom in Fig.3) taking (a) m=p=0; (b) m=0.5, p=0; (c) m=0, p=0.5; and (d) m=p=0.3. Data (symbols) from [10].

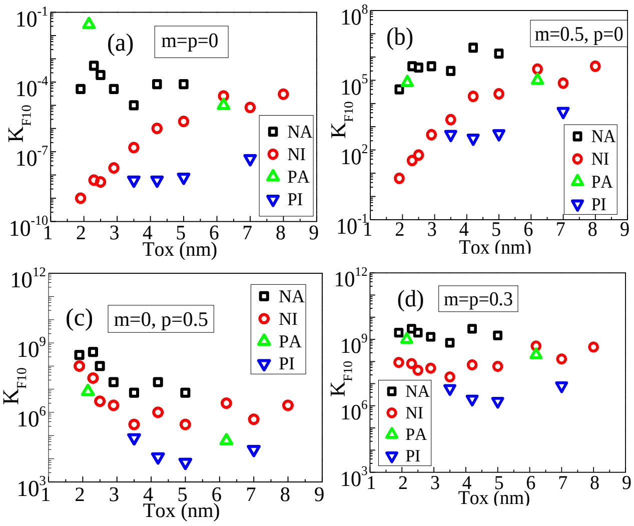

Fig.14 K_{F10} variation with oxide thickness (Tox) under various bias conditions with K_{F1} for (a) m=p=0 (b) m=0.5, p=0 (c) m=0, p=0.5 (d) m=p=0.3.

VI. COMPARISON OF END-OF-LIFE V_{GMAX}

The mean T_{BD} extrapolation up to 10 years (~$3.15\text{x}10^8$s) with gate voltage (V_G) from exponential-1/E law, exponential-E law, and V_G power law for 1.9nm NMOS capacitor in inversion at a constant T is illustrated in Fig.15(a) while those calculated from RDD simulations for different m and p values are shown in Fig.15(b). The maximum gate voltage (V_{GMAX}), corresponding to a mean T_{BD} of 10 years, versus Tox is shown in Fig.16(a) and Fig.16(b) respectively from extrapolation and RDD simulation. The exponential-1/E law projects the most optimistic V_{GMAX}, like AHI model (m=0, p=0.5), for all Tox's whereas exponential-E law turns out to be the most conservative. The TC model (m=p=0) becomes less optimistic at higher Tox's whereas AHR model (m=0.5, p=0) does so at lower Tox's. For all Tox's studied, the m=p=0.3 case shows a lesser optimistic but a consistent Tox dependence of V_{GMAX} values bounded by other cases. The variation of K_{F30} with Tox is shown in Fig.17 and the RDD parameters used are listed in Table-I. The tunneling electron leakage currents from Q_{BD} data [6], used for the RDD simulations, along with the leakage model [11] is shown in Fig.18.

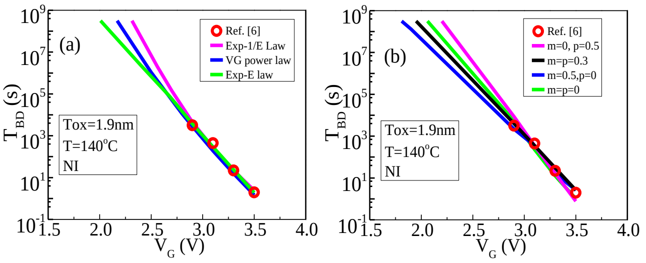

Fig.15 Illustration of gate bias extrapolation for 1.9nm up to 10 years (~$3\text{x}10^8$s) of mean T_{BD} from (a) exponential 1/E-law, exponential E-law, and V_G power law (b) RDD model simulation with m=p=0; m=0.5, p=0; m=0, p=0.5; and m=p=0.3. Data (symbols) from [6].

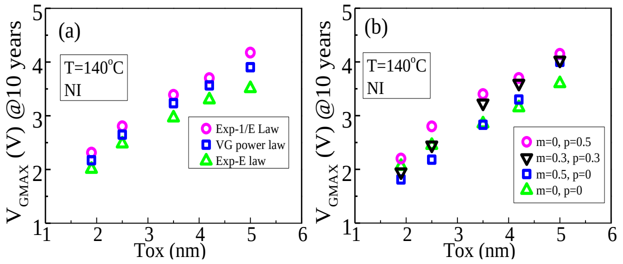

Fig.16 The maximum V_G variation with Tox for 10 years of mean T_{BD} from (a) exponential 1/E-law, exponential E-law, and V_G power law and (b) RDD simulation with m=p=0; m=0.5, p=0; m=0, p=0.5; and m=p=0.3.

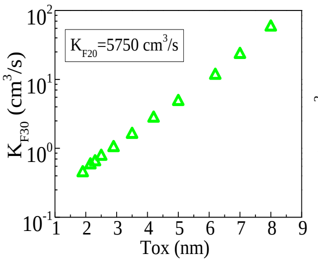

Fig.17 Variation of K_{F30} parameter of RDD model with oxide thickness Tox.

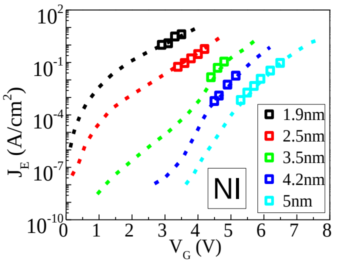

Fig.18 Tunneling leakage current variation with gate bias for various Tox. Symbols from Q_{BD}/T_{BD} data [6], dashed lines from tunneling model [11].

Table-I: RDD Model parameters

<table>
<tr><td colspan="4">K_{F10} and K_{F30} values are shown, respectively, in Fig.14 and Fig.17.
$N_{01}= N_{02}$ (cm^{-2})= 5% of N_A*Tox, N_A being the Avogadro number.
Fixed parameters: $K_{R10} = 5\times10^{-4} cm^3/s$, E_{AKR1}=0.12eV,
K_{F20}=5750 cm^3/s, E_{AKF2}=0.235 eV, K_{R20}=7.5e-4 cm^3/s, E_{AKR2}=0.2 eV</td></tr>
<tr><td>Tunneling leakage current exponent</td><td>E_{AKF1} (eV)</td><td>Γ_0 (cm/MV)</td><td>α (qÅ)</td></tr>
<tr><td>m=p=0</td><td>0.6</td><td>2.4</td><td>1.5</td></tr>
<tr><td>m=0.5, p=0</td><td>1.0</td><td>0.6</td><td>4.8</td></tr>
<tr><td>m=0, p=0.5</td><td>0.6</td><td>1</td><td>1.0</td></tr>
<tr><td>m=p=0.3</td><td>0.8</td><td>0.1</td><td>3.6</td></tr>
</table>

VII. CONCLUSION

RDD model is consistent with the requirement of reduction in ΔN_{TG} time slope *n* at lower Tox, in order to model Weibull β variation with Tox and SILC measurements. The V_G dependence of mean T_{BD} is successfully modelled across Tox and T, for different stress cases (NI, NA, PI, and PA). The co-injection of electrons and holes (from AHI), together with E_{OX} and T are found to be responsible for the initial trigger for the RDD model, leading to consistent set of model parameters across different Tox.

REFERENCES

[1] G. M. Paulzen, "Qbd dependencies of ultrathin gate oxides on large area capacitors," Microelectron. Eng., vol. 36, no. 1, pp. 321–324, Jun. 1997, doi: 10.1016/S0167-9317(97)00073-7.

[2] R. Degraeve, G. Groeseneken, R. Bellens, J.L. Ogier, M. Depas, P.J. Roussel, and H.E. Maes, "New insights in the relation between electron trap generation and the statistical properties of oxide breakdown," in *IEEE Transactions on Electron Devices*, vol. 45, no. 4, pp. 904-911, April 1998, doi: 10.1109/16.662800.

[3] T. Nigam, R. Degraeve, G. Groeseneken, M. M. Heyns, and H. E. Maes, "Constant current charge-to-breakdown: Still a valid tool to study the reliability of MOS structures?," *1998 IEEE International Reliability Physics Symposium Proceedings. 36th Annual (Cat. No.98CH36173)*, Reno, NV, USA, 1998, pp. 62-69, doi: 10.1109/RELPHY.1998.670444.

[4] T. Nigam, R. Degraeve, G. Groeseneken, M. M. Heyns, and H. E. Maes, "A fast and simple methodology for lifetime prediction of ultra-thin oxides," *1999 IEEE International Reliability Physics Symposium Proceedings. 37th Annual (Cat. No.99CH36296)*, 1999, pp. 381-388, doi: 10.1109/RELPHY.1999.761643.

[5] B. E. Weir, P.J. Silverman, M. A. Alam, F. Baumann, D. Monroe, A. Ghetti, J. D. Bude, G. L. Timp, A. Hamad, T. M. Oberdick, N. X. Zhao, Y. Ma, M. M. Brown, D. Hwang, T. W. Sorsch, and J. Madic, "Gate oxides in 50 nm devices: thickness uniformity improves projected reliability," *International Electron Devices Meeting 1999. Technical Digest (Cat. No.99CH36318)*, Washington, DC, USA, 1999, pp. 437-440, doi: 10.1109/IEDM.1999.824187.

[6] E. Wu, W. Lai, M. Khare, J. Sune, L. -K. Han, J. McKenna, R. Bolam, D. Harmon, and A. Strong, "Polarity-dependent oxide breakdown of NFET devices for ultra-thin gate oxide," *2002 IEEE International Reliability Physics Symposium. Proceedings. 40th Annual (Cat. No.02CH37320)*, Dallas, TX, USA, 2002, pp. 60-72, doi: 10.1109/RELPHY.2002.996611.

[7] E. Y. Wu, J. Sune, and W. Lai, "On the Weibull shape factor of intrinsic breakdown of dielectric films and its accurate experimental determination. Part II: experimental results and the effects of stress conditions," in *IEEE Transactions on Electron Devices*, vol. 49, no. 12, pp. 2141-2150, Dec. 2002, doi: 10.1109/TED.2002.805603.

[8] P. E. Nicollian, A. T. Krishnan, C. A. Chancellor, and R. B. Khamankar, "The Traps that cause Breakdown in Deeply Scaled SiON Dielectrics," *2006 International Electron Devices Meeting*, San Francisco, CA, USA, 2006, pp. 1-4, doi: 10.1109/IEDM.2006.346893.

[9] Y. Mitani, H. Satake, and A. Toriumi, "Impact of Deuterium and Fluorine Incorporation on Weibull Distribution Dielectric Breakdown in Gate Dielectrics," *ECS Transactions*, Volume 19, 2009, p.p 227-242. doi: 10.1149/1.3122094

[10] E. Y. Wu and J. Sune, "On Voltage Acceleration Models of Time to Breakdown—Part II: Experimental Results and Voltage Dependence of Weibull Slope in the FN Regime," in *IEEE Transactions on Electron Devices*, vol. 56, no. 7, pp. 1442-1450, July 2009, doi: 10.1109/TED.2009.2021725.

[11] E. Y. Wu, J. Sune, and R. -P. Vollertsen, "Comprehensive physics-based breakdown model for reliability assessment of oxides with thickness ranging from 1 nm up to 12 nm," *2009 IEEE International Reliability Physics Symposium*, 2009, pp. 708-717, doi: 10.1109/IRPS. 2009.5173335.

[12] Y. Mamy Randriamihaja, D. Garetto, V. Huard, D. Rideau, D. Roy, M. Rafik and A. Bravaix, "New insights into gate-dielectric breakdown by electrical characterization of interfacial and oxide defects with reverse modeling methodology," *2012 IEEE International Reliability Physics Symposium (IRPS)*, 2012, pp. GD.7.1-GD.7.5, doi: 10.1109/IRPS. 2012.6241914.

[13] E. Y. Wu and J. Sune, "Generalized hydrogen release-reaction model for the breakdown of modern gate dielectrics," *Journal of Applied Physics* 114, no. 1 (2013): 014103. doi: 10.1063/1.4811460

[14] K. F. Schuegraf and C. Hu, "Hole injection SiO_2 breakdown model for very low voltage lifetime extrapolation," in *IEEE Transactions on Electron Devices*, vol. 41, no. 5, pp. 761-767, May 1994, doi: 10.1109/16.285029.

[15] M. A. Alam, J. Bude, and A. Ghetti, "Field acceleration for oxide breakdown-can an accurate anode hole injection model resolve the E vs. 1/E controversy?," *2000 IEEE International Reliability Physics Symposium Proceedings. 38th Annual (Cat. No.00CH37059)*, San Jose, CA, USA, 2000, pp. 21-26, doi: 10.1109/RELPHY.2000.843886.

[16] J. W. McPherson and H. C. Mogul, "Underlying physics of the thermochemical E model in describing low-field time-dependent dielectric breakdown in SiO_2 films", *J. of App. Phys.*, vol. 84, no. 3, pp. 1513 – 1523, 1998, doi: 10.1063/1.368217.

[17] D. J. DiMaria and J. W. Stasiak, "Trap creation in silicon dioxide produced by hot electrons," *J. Appl. Phys.*, vol. 65, no. 6, pp. 2342-2356, 1989, doi: 10.1063/1.342824.

[18] D. J. Bude, B. E. Weir and P. J. Silverman, "Explanation of stress-induced damage in thin oxides," *International Electron Devices Meeting 1998. Technical Digest (Cat. No.98CH36217)*, San Francisco, CA, USA, 1998, pp. 179-182, doi: 10.1109/IEDM.1998.746313.

[19] J. Sune, S. Tous and E. Y. Wu, "Analytical Cell-Based Model for the Breakdown Statistics of Multilayer Insulator Stacks," in *IEEE Electron Device Letters*, vol. 30, no. 12, pp. 1359-1361, Dec. 2009, doi: 10.1109/LED.2009.2033617.

[20] E. Wu, E. Nowak and Wing Lai, "Off-state mode TDDB reliability for ultra-thin gate oxides: New methodology and the impact of oxide thickness scaling," *2004 IEEE International Reliability Physics Symposium. Proceedings*, Phoenix, AZ, USA, 2004, pp. 84-94, doi: 10.1109/RELPHY.2004.1315306.

[21] P. E. Nicollian, A. T. Krishnan, C. A. Chancellor, R. B. Khamankar, S. Chakravarthi, C. Bowen, and V. K. Reddy, "The Current Understanding of the Trap Generation Mechanisms that Lead to the Power Law Model for Gate Dielectric Breakdown," *2007 IEEE International Reliability Physics Symposium Proceedings. 45th Annual*, Phoenix, AZ, USA, 2007, pp. 197-208, doi: 10.1109/RELPHY.2007.369892

[22] K. Okada, H. Kubo, A. Ishinaga, and K. Yoneda, "A new prediction method for oxide lifetime and its application to study dielectric breakdown mechanism," *1998 Symposium on VLSI Technology Digest of Technical Papers (Cat. No.98CH36216)*, Honolulu, HI, USA, 1998, pp. 158-159, doi: 10.1109/VLSIT.1998.689239.

[23] A. Ghetti, J. Bude and G. Weber, "T/sub BD/ prediction from measurements at low field and room temperature using a new estimator," *2000 Symposium on VLSI Technology. Digest of Technical Papers (Cat. No.00CH37104)*, Honolulu, HI, USA, 2000, pp. 218-219, doi: 10.1109/VLSIT.2000.852832.

[24] P. E. Nicollian, A. T. Krishnan, C. Bowen, S. Chakravarthi, C. A. Chancellor, and R. B. Khamankar, "The roles of hydrogen and holes in trap generation and breakdown in ultra-thin SiON dielectrics," *IEEE International Electron Devices Meeting, 2005. IEDM Technical Digest.*, Washington, DC, USA, 2005, pp. 392-395, doi: 10.1109/IEDM. 2005.1609360.